FUDMA Journal of Sciences (FJS)
ISSN online: 2616-1370
ISSN print: 2645 - 2944
Vol. 10 No. 7, April, 2026, pp 357 – 365
DOI: https://doi.org/10.33003/fjs-2026-1007-4755

MATHEMATICAL MODELLING OF HEPATITIS E REVEALING THE NEMESIS OF HUMAN MOBILITY

[1]Agada Apeh Andrew, [2]Kifayah Tomilola Alabi, *[2]James Andrawus, [3]Rakiya Mohammed Ngoshe, [2]Felix Yakubu Eguda, [4]Danat Nanle, [5]Oghenefejiro Akpodamure, [6]Sunday Babuba, [2]Bashari Abdullahi, [7]Kefas Bitrus, [8]Stephen Ishaya Maiwa, [2]Oladele Yusuf Olatunji and [9]Ballah Akawu Denue

[1]Department of Mathematics, Prime University Abuja, Nigeria
[2]Department of Mathematics, Federal University Dutse, 7156 Jigawa, Nigeria
[3]Department of Medicine, Nile University Abuja, Nigeria
[4]Department of Mathematics, Plateau State University, Bokkos, Nigeria
[5]Department of Statistics, Federal Polytechnic Orogun, Delta State, Nigeria
[6]Department of Mathematics, Federal University of Agriculture Mubi, Nigeria
[7]Department of Mathematics, Federal University Lokoja, Nigeria
[8]Department of Mathematics, Federal University Birnin Kebbi, Nigeria
[9]Department of Medicine, University of Maiduguri, Nigeria

* Corresponding authors' email: james.a@fud.edu.ng

ABSTRACT

The hepatitis E virus causes hepatitis E, which is an outbreak of the liver. It is enteric in origin and is primarily spread orally, although it can also be spread through contaminated food, drink, and excrement. This work developed a novel model to study the impact of human mobility on hepatitis E virus dynamics; the reproduction number was calculated using a new generation matrix. Further, we calculated the disease-free equilibrium point of the model. The derived model has been fitted using Nigerian hepatitis E data, and a few parameters have been estimated using these data. Local sensitivity analysis has been conducted on the effective reproduction number, revealing that treatment is effective at reducing it, and that the effective contact rate is the most sensitive to increasing it. In this work, a numerical simulation has also been done.

Keywords: Hepatitis E, Mathematical Modeling, Human Mobility, Reproduction Number

INTRODUCTION

Hepatitis E is an inflammation of the liver caused by the hepatitis E virus. It is transmitted majorly via the oral route, it is enteric in nature (Hoofnagle *et al*. 2012),) and it can also be transmitted by contaminated foods, water, and infected stool (Yamashita *et al*. 2009). It is a waterborne severe infection, which is self-limiting and clears in 2-6 weeks. The history of the disease as an epidemiology emerges as an extrahepatic indication associated with hepatitis E infection, according to Jemersic *et al.* (2019). The World Health Organization statistics show that hepatitis E infects up to 20 million people per year in developing countries. The disease is minor but more severe in less developing countries due to limited access to a good water supply and poor hygiene (Sherman *et al.* 2018).

Hepatitis E virus is similar to hepatitis A virus, there are four genotypes of HEV, genotypes 1 and 2 are mainly related to waterborne, genotype 3 and genotype 4 appear to be common in animals, genotype 3 infections occur primarily in pigs, it is common in developed countries due to their consumption of the animals, it is asymptomatic in an immunocompetent patient, though, patient who contacted HEV infection after transplantation could develop chronic liver cirrhosis during immunosuppression, further delay could lead to advanced liver cirrhosis Puchhammer-stockl*et al*(2021).

The Hepatitis E virus is an RNA virus, although there has been no proof that the HEV strain can be transmitted from birds to humans. HEV1 and HEV2 predominantly contaminate young adults in the age bracket (15-30) in emerging countries, most cases of hepatitis E virus are asymptomatic, and orthohepevirus A HeV species also infect humans and mammals, the prodromal phase exists for a few weeks and a further progress to an icteric phase that could lead to acute liver damage (Lhomme *et al.,* 2020).

Pregnant women are at higher risk, HEV1 and HEV2 are responsible for acute hepatitis in pregnant women, ribavirin and interferon-alpha are some of the agents used in the treatment of the hepatitis E virus, although ribavirin is contraindicated in pregnant women (Aslan *et al.,* 2020).

Neurological disorders have frequently been documented in patients with severe or chronic hepatitis E virus infections, approximately 150 cases of neurological injury in HEV1-infected Asian and HEV3-infected (European *et al.,* 2016)

In March 2024, the World Health Organization was notified of a sudden outbreak of hepatitis E virus by Chad's International Health Regulation (IHR) nation focal point(NFP) with a large number of refugees and returnees, mostly women and children, have been flooding into Ouaddai province since April 2023 as a result of the crisis in Sudan. Between January 2, 2024, and April 28, 2024, two health districts in the province of Ouaddai, Adré, and Hadjer-Hadid, reported 2092 probable cases of hepatitis E, including seven fatalities (case fatality ratio, or CFR, of 0.3 percent, the host community accounted for 103, 4.9% of the 2092 suspected cases, while seven refugee camps and transit locations reported 1989 95 percent of the cases.

Mathematical modeling has been a critical mechanism for the discernment and development of effective intervening strategies. Osman *et al.* (2013) formulated a mathematical model using a fractional order derivative to study the transmission route of HEV as a zoonotic disease. Ren *et al.* (2013) reviewed the development of a combined mathematical model to forecast the incidence of hepatitis E in Shanghai, China, using an auto-regressive integrated moving average model(ARIMA) and a backpropagation neural network. Kontarov *et al.* (2019) formulated a mathematical model for developing hepatitis E virus infection in the human population based on the disease course, which may potentially predict an incidence rate for the most dangerous icteric HEV.

Khan *et al.* (2019) model the dynamics of HEV via the Caputo-Fabrizio derivative by the application of fixed point theory to obtain the basic properties of the model. Prakasha *et al*. (2019) analyses the dynamics of HEV using the fractional mathematical model of HEV using fractional Atangana Baleanu derivatives, their investigation shows the dynamics of the HEV model regarding time. Mwaijande *et al*. (2023) formulated a mathematical model for epidemiological hepatitis A with dual transmission mechanisms, Routh stability criteria were used to derive the stability of the model, and their model exhibits a forward bifurcation. Aniji *et al*. (2020) analyses how the number of infected cells and liver damage can be reduced. Lhomme *et al.* (2020) review recent advances in understanding the pathophysiology of acute HEV infections, including patients with severe liver disease with pre-existing liver disease and pregnant women.

The impact of human mobility on the disease cannot be over emphasized; this study aims to explore the dynamics of hepatitis E transmission dynamics using a deterministic model that integrates the dynamics of human mobility; According to our research, the impact of mobility on the spread of HEV has not been explicitly studied yet, due to the fact that the primary mode of transmission is fecal-oral, through contaminated water and food, it diagnosis is often overlooked due to its nonspecific symptoms. This research addresses the gap by introducing human mobility on the hepatitis E virus using patches to denote different regions in the model framework. Various sections were used to show the deterministic model factoring human mobility dynamics in spread, analysis of the disease-free equilibrium, computation of the basic reproduction number, formulation of the optimal control, numerical simulations, parameter fittings, and detailed conclusion of the research carried out.

This is how the research is structured: Section 2 contains the model formulation and model analysis; section 3 contains the model fitting and contains the sensitivity analysis; Section 4 contains the numerical illustration of the dynamic model; Section 5 contains the conclusion.

MATERIALS AND METHODS

Model formulation

Using a mathematical model approach, our model chooses the SPIR model for the sake of clarity, disregarding the convalescent phase. We introduce a multiple-patch vector host mathematical model focusing on a two-patch configuration of different locations or regions. Patches 1 and 2 were used to denote the locations or regions in this study with interactions and disease transmission due to human mobility, suggesting that the patches could intersect. Our model aims to show the interaction of the disease in the patches. We formulate a model based on the framework outlined by Hassan *et al*(2020). The convalescent phase of hepatitis E is the period when the body recovers from the illness and symptoms begin to resolve. While the symptoms from the prodromal or icteric phases (like jaundice) typically subside, low-grade fatigue or malaise may linger for a few weeks or even months. The body is gradually recovering, and the infection is usually self-limiting, meaning it resolves on its own without specific treatment. Based on the above explanation, we disregard the convalescent phase, the fact that they can recover without treatment at this stage. Further, in the formulation of the model, we considered two patches to study it using ordinary differential equations. Note that we did not intend to use stochastic approaches. Considering the above reasons leads to consideration of susceptible, prodromal, infected, and recovered individuals $SPIR$ in only two patches or cities.

$$
\begin{aligned}
N_1 &= S_1 + P_1 + I_1 + R_1 \\
N_2 &= S_2 + P_2 + I_2 + R_2 \\
S_1(0) &\geq 0, P_1(0) \geq (0), I_1(0) \geq 0, R_1(0) \geq 0 \\
S_2(0) &\geq 0, P_2(0) \geq (0), I_2(0) \geq 0, R_2(0) \geq 0 \\
\frac{dS_1}{dt} &= \pi_1 - \mu S_1 - \left(\frac{\beta_1(q_{11}(I_1+\eta P_1)+q_{12}(I_2+\eta P_2))}{q_{11}N_1+q_{12}N_2}\right) S_1, \\
\frac{dP_1}{dt} &= \left(\frac{\beta_1(q_{11}(I_1+\eta P_1)+q_{12}(I_2+\eta P_2))}{q_{11}N_1+q_{12}N_2}\right) S_1 - \sigma P_1 - \mu P_1, \\
\frac{dI_1}{dt} &= \sigma P_1 - \gamma I_1 - \mu I_1, \\
\frac{dR_1}{dt} &= \gamma I_1 - \mu R_1, \\
\frac{dS_2}{dt} &= \pi_2 - \mu S_2 - \left(\frac{\beta_2(q_{21}(I_1+\eta P_1)+q_{22}(I_2+\eta P_2))}{q_{21}N_1+q_{22}N_2}\right) S_2, \\
\frac{dP_2}{dt} &= \left(\frac{\beta_2(q_{21}(I_1+\eta P_1)+q_{22}(I_2+\eta P_2))}{q21N_1+q_{22}N_2}\right) S_2 - \sigma P_2 - \mu P_2, \\
\frac{dI_2}{dt} &= \sigma P_2 - \gamma I_2 - \mu I_2, \\
\frac{dR_2}{dt} &= \gamma I_2 - \mu R_2
\end{aligned} \tag{1}
$$

Subject to the initial condition;

$$
\begin{aligned}
&S_1(0) > 0, \quad P_1(0) \geq 0, \quad I_1(0) \geq 0, \quad R_1(0) \geq 0, \\
&S_2(0) \geq 0, \quad P_2(0) \geq 0, \quad I_2(0) \geq 0, \quad R_2(0) \geq 0.
\end{aligned}
$$

Table 1: Interpretation of the state variables and parameters used in the model (1)

Variable	Description
N_1	Total population in patch 1
N_2	Total population in patch 2
S_1	Susceptible individuals in patch 1
S_2	Susceptible individuals in patch 2
P_1	Prodromal individuals in patch 1
P_2	Prodromal individuals in patch 2
I_1	Infected Individuals in Patch 1
I_2	Infected Individuals in patch 2
R_1l	Recovered individuals in patch 1
R_2	Recovered individuals in patch 2
Parameter	
π_1, π_2	Recruitment rate
μ	Natural mortality rate
σ	progression rate
γ	Recovery rate
$q_{ij}(i = 1,2, j = 1,2)$	Rate of mobility from patch i to patch
β_1, β_2	Effective contact rates between humans

Variable	Description
η	in patch 1 and 2 Modification parameter due to reduced infectiousness of Prodromal individuals.

Denoting the death rate as μ_1, μ_2 and γ_1, γ_2, as recovery rate.

$$\lambda_1 = \frac{\beta_1(q_{11}(I_1+\eta P_1)+q_{12}(I_2+\eta P_2))}{q_{11}N_1+q_{12}N_2}$$
$$\lambda_2 = \frac{\beta_2(q_{21}(I_1+\eta P_1)+q_{22}(I_2+\eta P_2))}{q_{21}N_1+q_{22}N_2} \quad (3)$$

represent the force of infections within the patches at time t influenced by time-dependent transmission rate denoted by β_1, β_2. q is used to incorporate the moving frequencies between patch 1 and patch 2. therefore $\left(q_{11}(I_1+\eta P_1)+q_{12}(I_2+\eta P_2)\right)$represent number of infected individuals at time t in patch 1 and $(q_{21}(I_1+\eta P_1)+q_{22}(I_2+\eta P_2)$ represent number of infected individual at time t in patch 2, change in size of the population is represented by $N_1 =$ The total population of patch 1 is

$$\frac{dN_1}{dt} = \frac{dS_1}{dt}+\frac{dP_1}{dt}+\frac{dI_1}{dt}+\frac{dR_1}{dt}$$
$$= \pi_1 - \mu N_1 \quad (4)$$
$$R_1 = N_1 - S_1 - I_1 - P_1$$

Likewise

$$\frac{dN_2}{dt} = \frac{dS_2}{dt}+\frac{dP_2}{dt}+\frac{dI_2}{dt}+\frac{dR_2}{dt}$$
$$= \pi_2 - \mu N_2 \quad (5)$$
$$R_2 = N_2 - S_2 - I_2 - P_2$$

Assuming total population is constant, with the above argument, we have $\pi_1 = \mu N_1$ and $\pi_2 = \mu N_2$ our existing model becomes,

$$\begin{aligned}
\frac{dS_1}{dt} &= \mu(N_1 - S_1) - \left(\frac{\beta_1(q_{11}(I_1+\eta P_1)+q_{12}(I_2+\eta P_2))}{q_{11}N_1+q_{12}N_2}\right)S_1,\\
\frac{dP_1}{dt} &= \left(\frac{\beta_1(q_{11}(I_1+\eta P_1)+q_{12}(I_2+\eta P_2))}{q_{11}N_1+q_{12}N_2}\right)S_1 - (\sigma+\mu)P_1,\\
\frac{dI_1}{dt} &= \sigma P_1 - (\gamma+\mu)I_1,\\
\frac{dS_2}{dt} &= \mu(N_2 - S_2) - \left(\frac{\beta_2(q_{21}(I_1+\eta P_1)+q_{22}(I_2+\eta P_2))}{q_{21}N_1+q_{22}N_2}\right)S_2,\\
\frac{dP_2}{dt} &= \left(\frac{\beta_2(q_{21}(I_1+\eta P_1)+q_{22}(I_2+\eta P_2))}{q_{21}N_1+q_{22}N_2}\right)S_2 - (\sigma+\mu)P_2,\\
\frac{dI_2}{dt} &= \sigma P_2 - (\gamma+\mu)I_2,
\end{aligned} \quad (6)$$

Disease Free Equilibrium and Basic Reproduction Number

Disease-free equilibrium is calculated as follows:

$$\mathcal{E}_0 = (S_1, P_1, I_1, S_2, P_2, I_2) = (N_1, 0, 0, N_2, 0, 0) \quad (7)$$

At the end of disease-free equilibrium calculation, we then calculate the basic reproduction number by computing the matrices of infected classes first Ibrahim *et al.,* (2024), Andrawus *et al.,* (2024a), Andrawus *et al.,* (2024b), Andrawus *et al.,* (2024c), Ahmad *et al.,* (2024), Andrawus *et al.,* (2023), the matrices of infected class *P* which is getting from the new infection and G is by multiplying the remaining transition elements by negative Danat *et al.,* (2025), Danat *et al.,* (2025a), Eguda *et al.,* (2025), Andrawus *et al.,* (2025d), Andrawus *et al.,* (2025e), which are given below

$$\mathrm{P} = \begin{Bmatrix} \frac{\beta_1(q_{11}(I_1+\eta P_1)+q_{12}(I_2+\eta P_2))}{q_{11}N_1+q_{12}N_2}S_1, \\ 0, \\ \frac{\beta_2(q_{21}(I_1+\eta P_1)+q_{22}(I_2+\eta P_2))}{q_{21}N_1+q_{22}N_2}S_2, \\ 0 \end{Bmatrix} \quad (8)$$

and

$$\mathrm{G} = \begin{Bmatrix} k_1 P_1 \\ -\sigma P_1 + (\gamma+\mu)I_1 \\ k_3 P_2 \\ -\sigma P_2 + (\gamma+\mu)I_2 \end{Bmatrix}. \quad (9)$$

we differentiate each model equation in (8) with respect to each infected variables we got (10)

$$P = \begin{pmatrix} \frac{\eta\beta_1 q_{11}}{q_{11N_1}+q_{12N_2}} & \frac{\beta_1 q_{11}}{q_{11N_1}+q_{12N_2}} & \frac{\eta\beta_1 q_{12}}{q_{11N_1}+q_{12N_2}} & \frac{\beta_1 q_{12}}{q_{11N_1}+q_{12N_2}} \\ 0 & 0 & 0 & 0 \\ \frac{\eta\beta_2 q_{21}}{q_{21N_1}+q_{22N_2}} & \frac{\beta_2 q_{21}}{q_{21N_1}+q_{22N_2}} & \frac{\eta\beta_2 q_{22}}{q_{21N_1}+q_{22N_2}} & \frac{\beta_2 q_{22}}{q_{21N_1}+q_{22N_2}} \\ 0 & 0 & 0 & 0 \end{pmatrix} \quad (10)$$

also, differentiating each model equation in (9) with respect to each infected variable, we got (11)

$$\mathcal{G} = \begin{pmatrix} k_1 & 0 & 0 & 0 \\ -\sigma & k_2 & 0 & 0 \\ 0 & 0 & k_3 & 0 \\ 0 & 0 & -\sigma & k_4 \end{pmatrix} \quad (11)$$

then we calculate the $\mathcal{G}^{-1}$, which is given by

$$\mathcal{G}^{-1} = \begin{pmatrix} {k_1}^{-1} & 0 & 0 & 0 \\ \frac{\sigma}{k_1 k_2} & {k_2}^{-1} & 0 & 0 \\ 0 & 0 & {k_3}^{-1} & 0 \\ 0 & 0 & \frac{\sigma}{k_3 k_4} & {k_4}^{-1} \end{pmatrix} \quad (12)$$

and $\mathcal{P}\mathcal{G}^{-1}$ is given as

$$\mathcal{P}\mathcal{G}^{-1} = \begin{pmatrix} \mathcal{R}_1 & \frac{\beta_1 q_{11}}{(q_{11N_1}+q_{12N_2})k_2} & \mathcal{R}_2 & \frac{\beta_1 q_{12}}{(q_{11N_1}+q_{12N_2})k_4} \\ 0 & 0 & 0 & 0 \\ \mathcal{R}_3 & \frac{\beta_2 q_{21}}{(q_{21N_1}+q_{22N_2})k_2} & \mathcal{R}_4 & \frac{\beta_2 q_{22}}{(q_{21N_1}+q_{22N_2})k_4} \\ 0 & 0 & 0 & 0 \end{pmatrix} \quad (13)$$

where

$$\mathcal{R}_1 = \frac{\eta\,\beta_1 q_{11}}{(q_{11}N_1+q_{12}N_2)k_1} + \frac{\beta_1 q_{11}\sigma}{(q_{11}N_1+q_{12}N_2)k_1 k_2},$$
$$\mathcal{R}_2 = \frac{\eta\,\beta_1 q_{12}}{(q_{11}N_1+q_{12}N_2)k_3} + \frac{\beta_1 q_{12}\sigma}{(q_{11}N_1+q_{12}N_2)k_3 k_4},$$
$$\mathcal{R}_3 = \frac{\eta\,\beta_2 q_{21}}{(q_{21}N_1+q_{22}N_2)k_1} + \frac{\beta_2 q_{21}\sigma}{(q_{21}N_1+q_{22}N_2)k_1 k_2},$$
$$\mathcal{R}_4 = \frac{\eta\,\beta_2 q_{22}}{(q_{21}N_1+q_{22}N_2)k_3} + \frac{\beta_2 q_{22}\sigma}{(q_{21}N_1+q_{22}N_2)k_3 k_4}.$$

Next, the eigenvalues of matrix (13), is given by

$$\begin{bmatrix} 0 \\ 0 \\ \frac{\mathcal{R}_4+\mathcal{R}_1+\sqrt{{\mathcal{R}_4}^2-2\mathcal{R}_4\mathcal{R}_1+{\mathcal{R}_1}^2+4\mathcal{R}_3\mathcal{R}_2}}{2} \\ \frac{\mathcal{R}_4+\mathcal{R}_1-\sqrt{{\mathcal{R}_4}^2-2\mathcal{R}_4\mathcal{R}_1+{\mathcal{R}_1}^2+4\mathcal{R}_3\mathcal{R}_2}}{2} \end{bmatrix} \quad (14)$$

Further, we then choose the maximum of matrix (14), which is given as

$$\mathcal{R}_c = \frac{\mathcal{R}_4+\mathcal{R}_1+\sqrt{{\mathcal{R}_4}^2-2\mathcal{R}_4\mathcal{R}_1+{\mathcal{R}_1}^2+4\mathcal{R}_3\mathcal{R}_2}}{2}$$

Epidemiological Meaning of $\mathcal{R}_c$

The number of new infections caused by hepatitis E-infected persons in a population made up of susceptible and under-control individuals is known as the control reproduction number, or $\mathcal{R}_c$. It is, in a specific sense, the quantity generated by an infected person in the presence of social restrictions.

Model Fitting

Accurately selecting parameter values and evaluating models are significant challenges in mathematical modeling with empirical data. It is frequently essential to estimate these parameter values because they cannot be immediately derived from the data that were collected. Certain parameters can be more easily calculated by examining the early phases of an epidemic and taking into account relevant demographic data. Reference values for these factors can also be found in the existing literature. However, relying solely on literary values might occasionally produce unexpected outcomes. These real-world uses can take place across a range of time periods, from days to years, and any mistakes made during data analysis could affect the results. Although there are many different approaches for estimating parameters, the least-squares method is the most widely used.

Despite the validation of many epidemiological models, parameter estimation remains a significant challenge. The parameters are computed using actual data and maintained within acceptable bounds in order for the HEV model to accurately depict HEV. Instead of using values from existing models that have been found in the literature, estimating parameters based on real patient data guarantees that they are unique to the model produced. The relevant parameters were assessed using the least squares curve fitting approach with patient data. This fit was performed using data from Nigeria from the WHO dashboard (ECDC, 2019), which covered the years 2011–2020. Despite the existence of many different approaches to parameter estimation, the least-squares method is still the most widely used option. Parameter estimation is still a significant challenge even with established models. We employed parameter estimation using actual data with realistic constraints to make sure that our suggested hepatitis E model appropriately captures reality. This method eliminates reliance on values from other models by producing parameter values unique to our model.

By minimizing the discrepancy between the observed infection data and the values derived by simulating the model's equations, which are determined using the following formula, the least-squares method operates: we will fit the data with only a single population model below

$$\frac{dS_1}{dt} = \pi_1 - \mu S_1 - \frac{\beta_1((I_1+\eta P_1)}{N_1} S_1,$$
$$\frac{dP_1}{dt} = \frac{\beta_1((I_1+\eta P_1)}{N_1} S_1 - \sigma P_1 - \mu P_1,$$
$$\frac{dI_1}{dt} = \sigma P_1 - \gamma I_1 - \mu I_1,$$
$$\frac{dR_1}{dt} = \gamma I_1 - \mu R_1,$$
$$\text{Residual} = \frac{1}{N}\sum_{j=0}^{N}\left|\frac{\hat{y}_j - y_j}{\hat{y}_j}\right|.$$

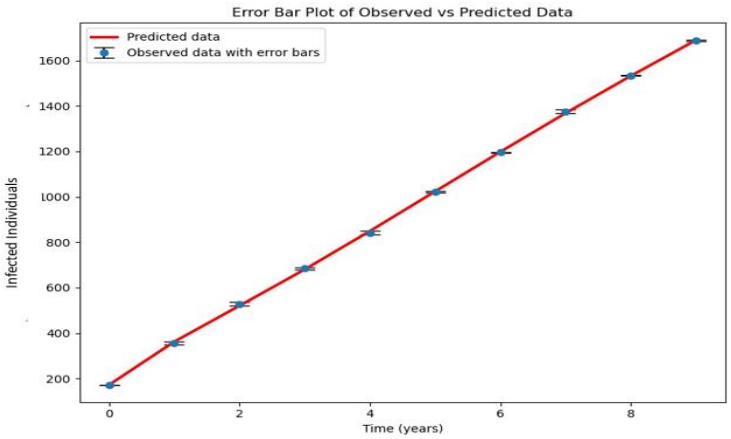

Figure 1: Comparison between the simulations produced using the suggested HEV model and actual HEV data of Nigeria

Table 2: Parameter values

Parameter	Value and Unit	Reference
π_1, π_2	$520{,}500 year^{-1}$	Andrawus *et al*., (2024c)
μ	$0.0324 year^{-1}$	Andrawus *et al*., (2024c)
σ	$0.09 year^{-1}$	fitted
γ	$0.53 year^{-1}$	fitted
β_1, β_2	$0.6321, 0.6432 year^{-1}$	fitted
η	0.421 dimensionless	estimated
q_{11}, q_{12}	$0.342, 0.437 year^{-1}$	estimated
q_{21}, q_{22}	$0.458, 0.497 year^{-1}$	estimated

Sensitivity Analysis

The sensitivity status of each parameter and its effect on limiting the spread of HEV in the specified population are determined by analyzing the suggested HEV model using the forward sensitivity index approach. The uncertainty that surrounds the model's parameters is what happens when we see specific parameters as potentially applicable for disease control, but turn out to be ineffective when examined for sensitivity to reproduction number. Additionally, there is uncertainty surrounding the model's parameters because we typically believe that some of them have the potential to be ineffective in controlling disease, but testing their sensitivity to reproduction number reveals that they are not. According to Andrawus *et al.,* (2022), the most sensitive parameters to increase and lower the value of $\mathcal{R}_c$ are represented by positive and negative signs, respectively. The normalized local sensitivity index of $\mathcal{R}_c$ with respect to the biological parameters of the model is expressed as:

$$\chi_m^{\mathcal{R}_c} = \frac{\mathcal{J}}{\mathcal{R}_c} \times \frac{\partial \mathcal{R}_c}{\partial \mathcal{J}},$$

Table 3: Forward Normalized Sensitivity Indices

Parameter	Elasticity Indices	Values of the Elasticity index
μ	$\chi_{\mu}^{\mathcal{R}_c}$	0.4923
δ_1	$\chi_{\delta_1}^{\mathcal{R}_c}$	-0.7115
δ_2	$\chi_{\delta_2}^{\mathcal{R}_c}$	0.4123
η	$\chi_{\eta}^{\mathcal{R}_c}$	0.31234
β_1	$\chi_{\beta_1}^{\mathcal{R}_c}$	0.9973
β_2	$\chi_{\beta_2}^{\mathcal{R}_c}$	0.9998
σ_1	$\chi_{\sigma_1}^{\mathcal{R}_c}$	0.3231
σ_2	$\chi_{\sigma_2}^{\mathcal{R}_c}$	0.4002
γ	$\chi_{\gamma}^{\mathcal{R}_c}$	-0.7425
p_{11}	$\chi_{p_{11}}^{\mathcal{R}_c}$	0.4231
p_{12}	$\chi_{p_{12}}^{\mathcal{R}_c}$	-0.5219
p_{21}	$\chi_{p_{21}}^{\mathcal{R}_c}$	0.3978
p_{22}	$\chi_{p_{22}}^{\mathcal{R}_c}$	-0.4869

Numerical illustration of the dynamic model

This section will address the numerical simulation part of this paper, especially the human mobility part and treatment. The influence of mobility will be checked on the infected classes of the proposed model.

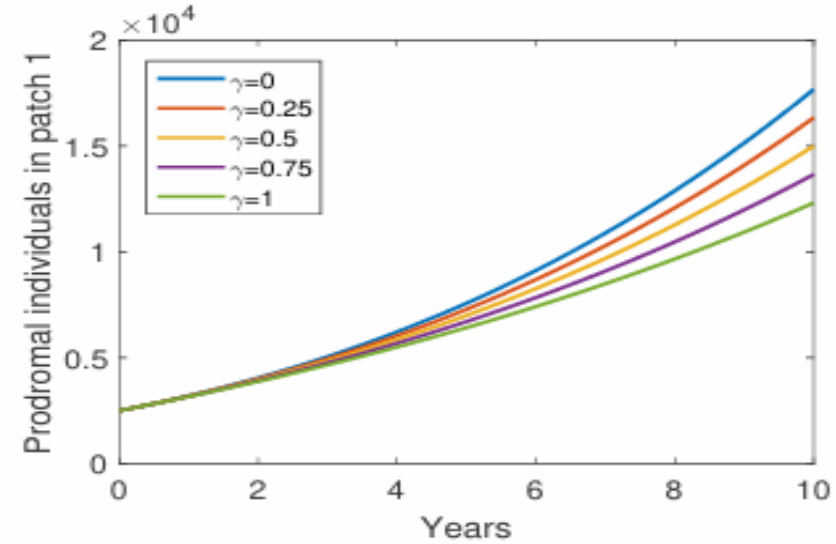

Figure 2: Influence of treatment on Prodromal individuals in patch 1

Figure 2 shows the influence of treatment on prodromal individuals in patch 1, it clearly shows that treatment helps control prodromal individuals in patch 1.

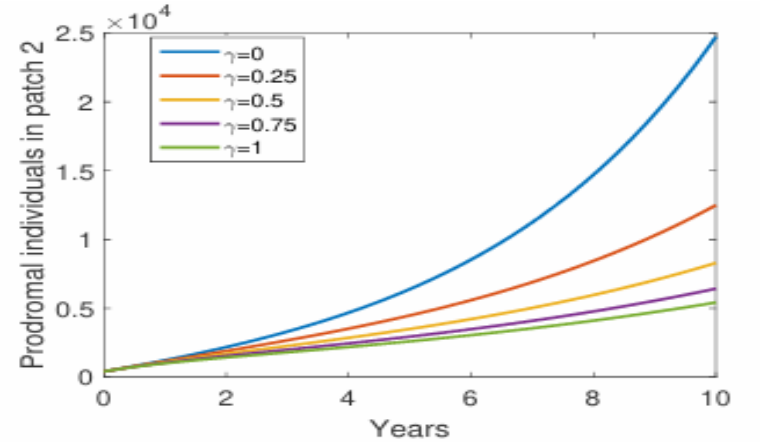

Figure 3: Influence of treatment on Prodromal individuals in patch 2

Figure 3 shows the influence of treatment on Prodromal individuals in Patch 2; it clearly indicates that treatment helps control them. Treating 25 per cent of Prodromal individuals in Patch 2 shows a great impact on the population of Prodromal individuals in Patch 2.

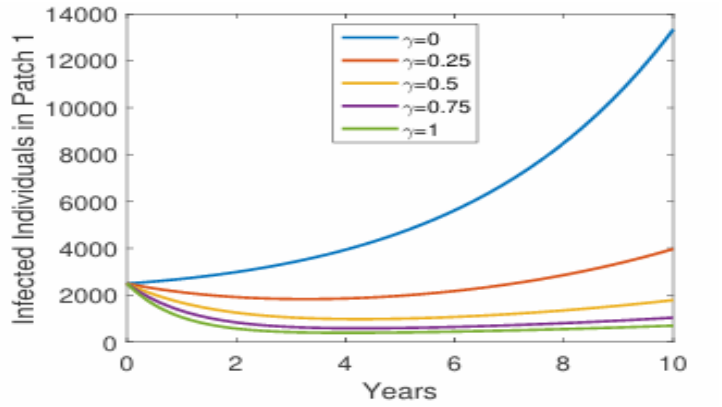

Figure 4: Influence of treatment on Infected Individuals in Patch 1

Figure 4 shows the influence of treatment on Infected Individuals in patch 1; it clearly indicates that treatment helps control them. Treating 25 per cent of Infected Individuals in Patch 1 shows a great impact on the population of Infected Individuals in Patch 1.

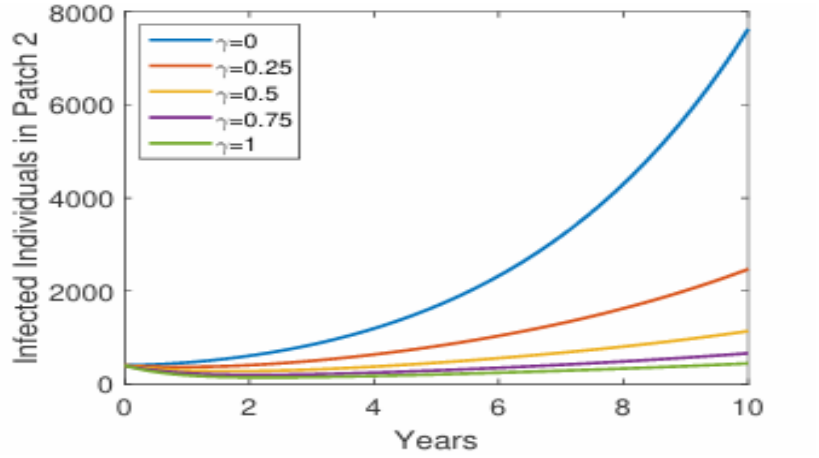

Figure 5: Influence of treatment on Infected Individuals in Patch 2

Figure 5 shows the influence of treatment on Infected Individuals in patch 2; it clearly indicates that treatment helps control them. Treating 25 per cent of Infected Individuals in Patch 2 has a significant impact on the population of Infected Individuals in Patch 2, nearly eradicating the disease in this population.

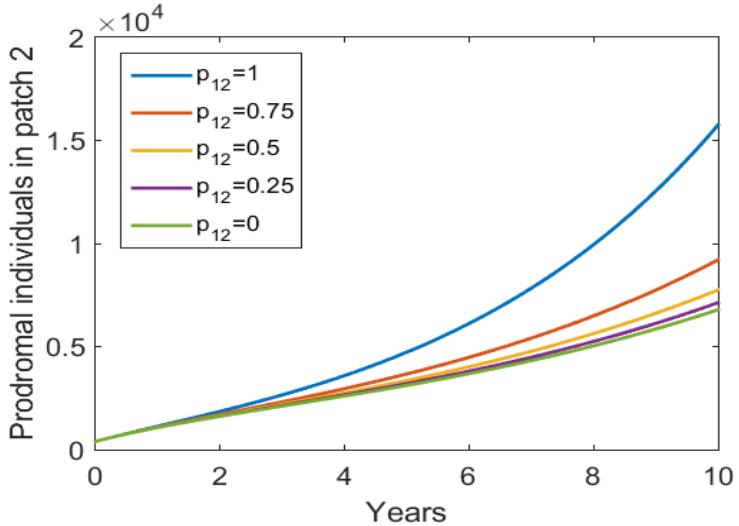

Figure 6: Influence of treatment on Prodromal individuals in patch 1

Figure 6 shows the influence of the mobility rate of patch 1 to patch 2 on Prodromal individuals in patch 1; it clearly shows that the mobility rate from patch 1 to patch 2 tends to increase Prodromal individuals in patch 1. Decreasing the mobility rate from patch 1 to patch 2 by 25 percent helps in reducing the Prodromal individuals in patch 1; this shows a great impact in decreasing the population of Prodromal individuals in patch 1.

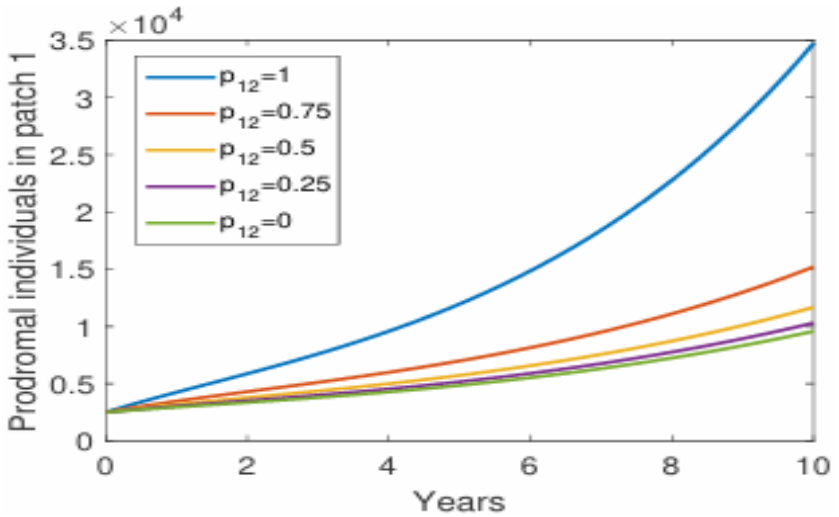

Figure 7: Influence of treatment on Prodromal individuals in patch 2

Figure 7 shows the influence of the mobility rate of patch 1 to patch 2 on Prodromal individuals in patch 2. It clearly shows that the mobility rate from patch 1 to patch 2 tends to increase the Prodromal individuals in patch 2. Decreasing the mobility rate from patch 1 to patch 2 by 25 percent helps in reducing the Prodromal individuals in patch 2. This shows a great impact in decreasing the population of Prodromal individuals in patch 2.

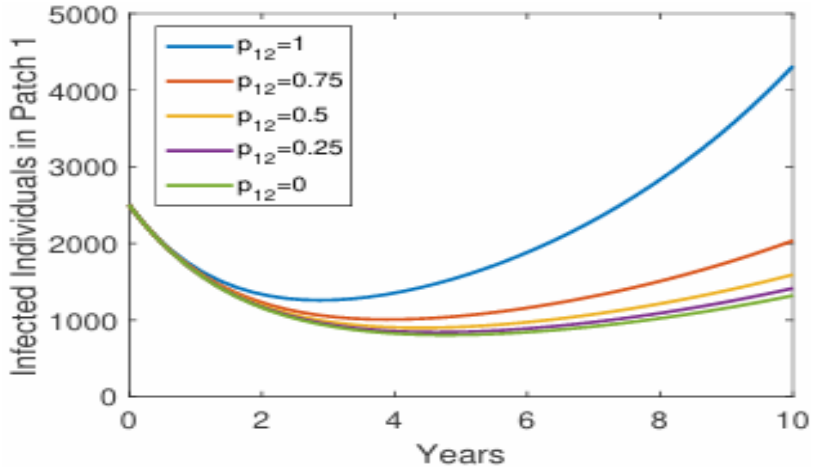

Figure 8: Influence of treatment on Infected Individuals in Patch 1

Figure 8 shows the influence of the mobility rate of patch 1 to patch 2 on infected individuals in patch 1, clearly showing that the mobility rate of patch 1 to patch 2 tends to increase infected individuals in patch 1. Decreasing the mobility rate from patch 1 to patch 2 by 25 percent helps in decreasing the infected individuals in patch 1, which shows a great impact in decreasing the population of infected individuals in patch 1.

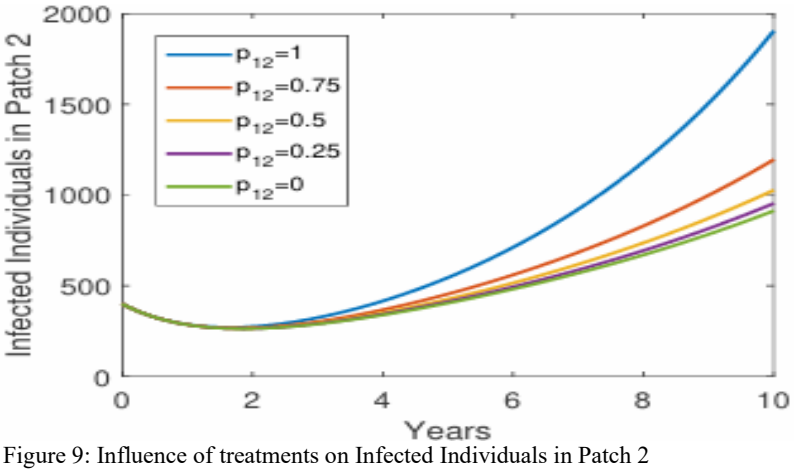

Figure 9: Influence of treatments on Infected Individuals in Patch 2

Figure 9 shows the influence of the mobility rate of patch 1 to patch 2 on infected individuals in patch 2, clearly showing that the mobility rate of patch 1 to patch 2 tends to increase infected individuals in patch 2. Decreasing the mobility rate from patch 1 to patch 2 by 25 per cent reduces the number of infected individuals in patch 2, indicating a significant impact on its population.

CONCLUSION

This work developed a novel model to study the impact of human mobility on the dynamics of hepatitis E virus; the reproduction number and the disease-free equilibrium have been calculated. The proposed model has been fitted using Nigerian hepatitis E data, and a few parameters have been estimated using these data. A local sensitivity analysis of the effective reproduction number has been performed, showing that treatment is sensitive to reducing it, and that effective contact rates are the most sensitive to increasing it. Numerical simulation reveals that a decrease in human mobility will help eradicate the disease. It is therefore recommended to reduce mobility whenever suspected cases are found in society; measures must be taken before allowing mobility in and out of society. Further studies need to be done on hepatitis E by considering multiple patches to enhance control further.

REFERENCES

Abdullah Tarık Aslan, Hatice Yasemin Balaban (2020) Hepatitis E virus: Epidemiology, diagnosis, clinical manifestations, and treatmentAffiliations Expand PMID: 33071523 PMCID: PMC7545399 https://doi.org/10.3748/wjg.v26.i37.5543

Ahmad, Y. U., Andrawus, J., Ado, A., Maigoro, Y. A., Yusuf, A., Althobaiti, S., & Mustapha, U. T. (2024). *Mathematical modeling and analysis of human-to-human monkeypox virus transmission with post-exposure vaccination*. Modeling Earth Systems and Environment, 1-21. https://doi.org/10.1007/s40808-023-01920-1

Andrawus, J., Abdulrahman, S., Singh, R.V.K. and Manga, S.S. (2022) Sensitivity Analysis of Mathematical Modeling of Ebola Virus Population Dynamics in the Presence of Vaccine. DUJOPAS. 8(2a):40-46. https://dx.doi.org/10.4314/dujopas.v8i2a.5

Andrawus, J., Abubakar, A., Yusuf, A. et al. Impact of public awareness on haemo-lyphatic and meningo-encepphalitic stage of sleeping sickness using mathematical model approach. Eur. Phys. J. Spec. Top. (2024a). https://doi.org/10.1140/epjs/s11734-024-01417-7

Andrawus, J., Iliyasu Muhammad, A., Akawu Denue, B., Abdul, H., Yusuf, A., & Salahshour, S. (2024c). Unraveling the importance of early awareness strategy on the dynamics of drug addiction using mathematical modeling approach. Chaos: An Interdisciplinary Journal of Nonlinear Science, 34(8). https://doi.org/10.1063/5.0203892

Elisabeth Puchhammer-Stockl,Fausto Baldanti (2021) Virus Diagnosis in Immunosuppressed Individuals. https://doi.org/10.1016/B978-0-12-814515-9.00125-9

Danat Nanle Tanko, Farah Aini Abdullah, Majid Khan, Matthew O. Adewole, and James Andrawus. (2025) Onchocerciasis control via Caputo-Fabrizio fractional dynamics: a focus on early treatment and vector management strategies. *J. Nig. Soc. Phys. Sci.* 7 (2025) 2618

Danat Nanle Tanko, Farah Aini Abdullah, Majid Khan, Matthew O. Adewole, and James Andrawus. (2025a) Analyzing Onchocerciasis Transmission Dynamics through Mathematical Models Incorporating Early Therapeutic Intervention and Vector Control. *IAENG International Journal of Applied Mathematics*, 55(11); 3579-3599.

European Centre for Disease Prevention and Control.HIV infection and AIDS. In: ECDC. Annual epidemiologica report for 2018. Stockhom ECDC; 2019 https://www.ecdc.europa.eu/en/publications-data/hivaids-surveillance-europe-2019-2018-data

Felix Yakubu Eguda, James Andrawus, Sadiya Ufeli Balogun, & Maryann Ufedo Eguda. (2025). Predicting the impact of education on malaria transmission with sensitivity analysis and optimal control. Dutse Journal of Pure and Applied Sciences, 11(3d), 359–381. https://doi.org/10.4314/dujopas.v11i3d.33

Hong Ren , Jian Li , Zheng-An Yuan , Jia-Yu Hu , Yan Yu and Yi-Han Lu (2013) The development of a combined mathematical model to forecast the incidence of hepatitis E in Shanghai, China. PMCID: PMC3847129 PMID: 24010871 https://doi.org/10.1186/1471-2334-13-421

Hoofnagle JH Nelson KE, Purcell RH.Hepatitis E.N Engl J Biological and immunological characteristics of hepatitis E virus-like particles based on the crystal structure. Med.2012

Sep 27;367(13):1237-44. https://doi.org/10.1056/NEJMra1204512.PMID:23013075

Ibrahim, K.G., Andrawus, J., Abubakar, A. et al. Mathematical analysis of chickenpox population dynamics unveiling the impact of booster in enhancing recovery of infected individuals. Model. Earth Syst. Environ. 11, 46 (2025). https://doi.org/10.1007/s40808-024-02219-5

James Andrawus, Abdullahi Yusuf, Umar Tasiu Mustapha, Ali S. Alshom-rani, Dumitru Baleanu. (2023). Unravelling the Dynamics of Ebola Virus with Contact Tracing as Control Strategy. Fractals, 31, 10 https://doi:10.1142/S0218348X2340159X

J. Andrawus, J. Y. Musa, S. Babuba, A. Yusuf, S. Qureshi, U. T. Mustapha, A. Oghenefejiro, I. S. Mamba (2025d). Modeling the dynamics of pertussis to assess the influence of timely awareness with optimal control analysis. J. Nig. Soc. Phys. Sci. 7 (2025) 2732. https://doi.org/10.46481/jnsps.2025.2732

James Andrawusa, Kayode Isaac Omotoso, Agada Apeh Andrew, Felix Yakubu Eguda, Sunday Babuba, Kabiru Garba Ibrahim. (2025e) Mathematical model analysis on the significance of surveillance and awareness on the transmission dynamics of diphtheria. J. Nig. Soc. Phys. Sci. 7 (2025) 2618. https://doi.org/10.46481/jnsps.2025.2618

Kenneth E.Sherman,Richard K.Sterling (2018) HIV and the Liver.Zakim and Bayer Hepatology (seventh edition). https://doi.org/10.1016/B978-0-323-37591-7.00037-9

Kontarov N.A., Yuminova N.V.,Alatortseva G.I.,Lukhverchik L.N.,Nurmatov Z.Sh.,Pogarskaya I.V.(2019) A mathematical model for developing hepatitis E virus infection in human population. Russian Journal of Infection and Immunity, 2019, vol. 9, no. 2,pp. 381–384. https://doi.org/10.15789/2220-7619-2019-2-381-384

Lorena Jemersic,Jelena Prpic,Dragan Brnic,Tomislav Keros,Nenad Pandak,Oktavija Dakovic Rode,(2019) Genetic diversity of hepatitis E virus (HEV) strains derived from humans, swine and wild boars in Croatia from 2010 to 2017 PMID: 30890143 PMCID: PMC6425696 https://doi.org/10.1186/s12879-019-3906-6

Muhammad Altaf Khan, Zakia Hammouch and Dumitru Baleanu (2019) Modeling the dynamics of hepatitis E via the Caputo–Fabrizio derivative: https://doi.org/10.1051/mmnp/2018074

Prakasha, D.G., Veeresha, P. and Baskonus, H.M. (2019). Analysis of the dynamics of hepatitis E virus using the Atangana-Baleanu fractional derivative. Eur. Phys. J. Plus 134, 241 (2019) https://doi.org/10.1140/epjp/i2019-12590-5

Saratu Midankiya Ezekiel, Sunday Babuba, Ibrahim Abba Bakari, James Andrawus, Stephen Ishaya Maiwa, Lawal Shehu Fakai, Jonathan Joseph. (2026). Mathematical Modeling for the Control and Management of Northern Corn Leaf Blight in Maize with Early Chemical Spray on Maize Plant. FUDMA Journal of Science

Sebastien Lhomme , Olivier Marion ,Florence Abravanel , Jacques Izopet , Nassim Kamar (2020)Clinical Manifestations, Pathogenesis and Treatment of Hepatitis E Virus Infections,PMCID: PMC7073673 PMID: 31991629 https://doi.org/10.3390/jcm9020331

Shaibu Osman, Binandam Stephen Lassong, Munkaila Dasumani, Ernest Yeboah Boateng, Winnie Mokeira Onsongo, Boubacar Diallo, Oluwole Daniel Makinde (2024).Modeling the Transmission Routes of Hepatitis E Virus as a Zoonotic Disease Using Fractional-Order Derivative https://doi.org/10.1155/2024/5168873.

Stephen Edward Mwaijande, Godfrey Edward Mpogolo(2023) Modeling the Transmission Dynamics of Hepatitis A with Combined Vaccination and Sanitation Mitigation https://doi.org/10.1155/2023/1203049

World Health Organisation /Disease outbreak News/item/Hepatitis E-Chad (2024). https://www.who.int/emergencies/emergency-events/item/2024-DON517

Yamashita T,Mori Y,Miyazaki N, Cheng RH,Yoshimura M,Unno H,Shima R,Moriishi K Tsukihara T,Li TC,Takeda N,Miyamura T,Matsuura Y Biological and immunological characteristics of hepatitis E virus-like particles based on the crystal structure.Proc Natl Acad Sci U S A.2009 Aug 4;106(31):12986-91. https://doi.org/10.1073/pnas.0903699106.